

APPLICABILITY OF TDLAS GAS DETECTION TECHNIQUE TO COMBUSTION CONTROL AND EMISSION MONITORING UNDER HARSH ENVIRONMENT

Hajime Arimoto^{1*}, Nobuo Takeuchi^{2,1}, Sachio Mukaiharu¹, Toru Kimura¹,
Ryuzo Kano¹, Takeo Ohira¹, Shinji Kawashima¹, Kazuya Iwakura¹

¹*Kyoto Electronics Manufacturing Co., Ltd*
74 Kisshoin Shinden Ninodan-cho, Minami-ku, Kyoto 601-8317, Japan
²*Center for Environmental Remote Sensing, Chiba University*
1-33 Yayoi-cho, Inage-ku, Chiba 263-8522, Japan

(Received: November 2010 / Revised: December 2010 / Accepted: January 2011)

ABSTRACT

Tunable diode laser absorption spectroscopy (TDLAS) has been well-known as an established detection technique for trace gas molecules and analytical instruments based on this technique are already commercially available. Practical applications to combustion control and emission monitoring for incinerators and industrial furnaces often involve considerations about the technique's capability to cope with such harsh measuring environmental conditions as high temperature, high pressure and high humidity. In this study, we theoretically describe the laser modulation spectroscopy technique and discuss practical applicability of the technique through a comparison between laboratory experimental results and theoretical calculations by the use of a molecular spectroscopic database, stressing on hydrogen chloride (HCl) measurement for exhaust gas of incinerators. Under experimental condition of elevated temperature, observed absorption line strength deduced by the second harmonic absorption spectrum of HCl in the first overtone region shows good agreement with theoretical prediction. This result indicates that variation of absorption signal due to temperature variation of flue gas can be compensated if gas temperature is simultaneously obtained.

Keywords: Combustion control; Emission monitoring; Hydrogen Chloride (HCl); Molecular spectroscopy; Tunable Diode Laser Absorption Spectroscopy (TDLAS)

1. INTRODUCTION

Exhaust trace gas concentration monitoring in an incinerator is important for avoiding air pollutions and also for combustion control and efficiency improvement. A trace gas concentration measurement technique making use of a laser diode (LD) has recently gained increased popularity since it does not require sampling of a flue gas and thus can easily perform real-time and *in situ* monitoring with less maintenance.

From the viewpoint of reducing the adverse influences of the circumstance to the measurement, the frequency modulation spectroscopy (FMS), or the wavelength modulation spectroscopy (WMS) has been preferably adopted. In WMS, the laser frequency is modulated at a much lower frequency than FMS.

* Corresponding author's email: arimoto.hajime@kyoto-kem.com, Tel. +81-75-691-9938, Fax. +81-75-691-2677

However, it is not easy to obtain the absolute concentration of the gas molecule of interest because FMS or WMS signals could be drastically affected depending on the ratio of the modulation amplitude to the half-width of the absorption spectrum, as well as on the temperature, pressure and humidity of the sample gas. In this paper, the fundamental theory of the FMS (WMS) method is briefly described and the FMS (WMS) signal is simulated. The laboratory experimental result of HCl (hydrogen chloride) measurement under the elevated gas temperature is compared with the theory, and the practical applicability of the FMS (WMS) technique to emissions monitoring and combustion control is discussed.

2. FREQUENCY MODULATION SPECTROSCOPY

In the strict mathematical treatment (Cooper & Warren, 1987), the electric field of the input signal of FMS can be written as

$$E_1(t) = E_0(t) \{1 + M_s \sin(2\pi ft + \psi)\} \exp(i\beta \sin 2\pi ft) \quad (1)$$

$$= E_0(t) \sum_{n=-\infty}^{\infty} r_n \exp(i2\pi nft) \quad (2)$$

where $E_0(t)$, f , M_s , β and ψ respectively denote the electric field amplitude of the carrier signal, the modulation frequency, the amplitude modulation factor, the frequency modulation amplitude and the phase difference between amplitude modulation and frequency modulation. In (1) and (2), the frequency of the carrier signal $\bar{\nu}$ is implicitly expressed in $E_0(t)$, and i is the imaginary unit. In (2), r_n denote the coefficients of the amplitude when the modulation frequency is expanded in Bessel series. In this treatment, Fourier transform of (2) is multiplied by the molecular absorption term $\exp(-\alpha/2 - i\phi)$, where α and ϕ respectively denote the molecular absorption coefficient and the phase shift by the sample medium, and then the resultant terms experience inverse Fourier transform. During this procedure, only necessary harmonic components have been picked out and the square of the amplitude of these components yields the FMS signal. Alternatively, the FMS signal can be obtained by the numerical Fourier transform of the transmitted signal (Uehara, 1998).

Our treatment in the present study follows Silver (1992), where the approximated description is valid on the assumption of the weak absorption. For the optically thin condition of a weak absorption, the transmitted light intensity can be written as:

$$\begin{aligned} I(\nu) &= I_0(\nu)T(\nu) = I_0(\nu) \exp(-\alpha(\nu)L) \\ &\approx I_0(\nu)(1 - \alpha(\nu)L) \quad \dots [\alpha(\nu)L \leq 0.05] \end{aligned} \quad (3)$$

where $I_0(\nu)$ is the incident laser intensity at the frequency ν and L is the optical path length (Reid & Labrie, 1983). As the angular frequency ω is the temporal derivative of the phase ϕ , $\omega(t)$ is given as follows.

$$\begin{aligned} \omega(t) &= \frac{d}{dt}(\bar{\omega}t + \beta \sin 2\pi ft) \\ &= \bar{\omega} + 2\pi\beta f \cos 2\pi ft = 2\pi(\bar{\nu} + a \cos 2\pi ft) \end{aligned} \quad (4)$$

Here $\bar{\nu}$ and $\bar{\omega}$ are respectively the frequency and the angular frequency of the incident laser light, and $a = \beta \square f$. When we assume the incident laser intensity is independent of the laser frequency in the vicinity of resonant frequency ν_0 of the target gas, then

$$I_0(\nu) \approx I_0(\nu_0) \approx I_0 \quad (5)$$

Using the relationships (Reid & Labrie, 1983; Wilson, 1963) of

$$\alpha(\bar{\nu} + a \cos 2\pi ft) = \sum_{k=0}^{\infty} H_k(\bar{\nu}, a) \cos(k2\pi ft) \quad (6)$$

and

$$I(t) = I_0(t)T(\nu(t)) = I_0(t) \left\{ 1 - L \sum_{k=0}^{\infty} H_k(\bar{\nu}, a) \cos(k2\pi ft) \right\} \quad (7)$$

where $T(\nu(t))$ is the transmission coefficient and $H_k(\bar{\nu}, a)$ is the Fourier component of absorption coefficient $\alpha(\bar{\nu} + a \cos 2\pi ft)$, the n -th order higher frequency is written as

$$I_0 H_n(\bar{\nu}) L \quad (n \geq 1) \quad (8)$$

Here $H_n(\bar{\nu})$ is given as

$$H_n(\bar{\nu}) = \frac{2^{1-n}}{n!} a^n \left. \frac{d^n \alpha(\nu)}{d\nu^n} \right|_{\nu=\bar{\nu}} \quad (n \geq 1) \quad (9)$$

For the uniform gas concentration with Lorentzian absorption line shape under uniform temperature and pressure along the optical path, the absorption is given as

$$\alpha(\nu)L \approx \int_0^L PXS\Phi dx \approx (XL)PS\Phi \quad (10)$$

$$\approx (XL)PS \left\{ \frac{2}{\pi \Delta\nu_c} \frac{1}{1 + (x + m \cos(2\pi ft))^2} \right\} \quad (11)$$

Here P is the total pressure, X is the concentration (the partial pressure) of the target gas, S is the absorption line strength, Φ is the spectral distribution function and $\Delta\nu_c$ is the full width at half maximum (FWHM) of the absorption spectrum. Also x and m are set as

$$x = \frac{\bar{\nu} - \nu_0}{\Delta\nu_c/2}, \quad m = \frac{a}{\Delta\nu_c/2} \quad (12)$$

where m is the modulation index.

The Fourier coefficient was calculated by Wahlquist (1961) and Arndt (1965). For the second harmonic frequency, Fourier coefficient $H_2(x, m)$ is expressed as:

$$H_2(x, m) = \frac{\sqrt{2}}{m^2} \left\{ \frac{(M+1-x^2)}{\sqrt{M^2+4x^2}} \right\} \left(\sqrt{M+\sqrt{M^2+4x^2}} + 4x\sqrt{\sqrt{M^2+4x^2}-M} \right) - \frac{4}{m^2} \quad (13)$$

where $M = 1 - x^2 + m^2$, and the second harmonic frequency signal is given as

$$2f \text{ signal} \propto \frac{2(XL)PS}{\pi\Delta\nu_c} H_2(x, m) \quad (14)$$

Figure 1(a) illustrates the calculated second harmonic frequency signal for the modulation index $m = 1, 2, 3, 4$ and 5 . As shown in the figure, the shape of $H_2(x, m)$ traces are varied depending on the modulation index, i.e., on the ratio of the modulation amplitude to the half-width at half maximum (HWHM) of the absorption spectrum. Figure 1(b) apparently shows the peak height of $H_2(x, m)$ dependence on the modulation index. The inset explains the definition of the peak height P and the separation between the peak and the trough (the extreme minimum) $P+N$ of the second harmonic absorption signal. The peak height P has its maximum at $m \sim 2.2$, while the separation between the peak and the trough $P+N$ appears at $m \sim 3.1$.

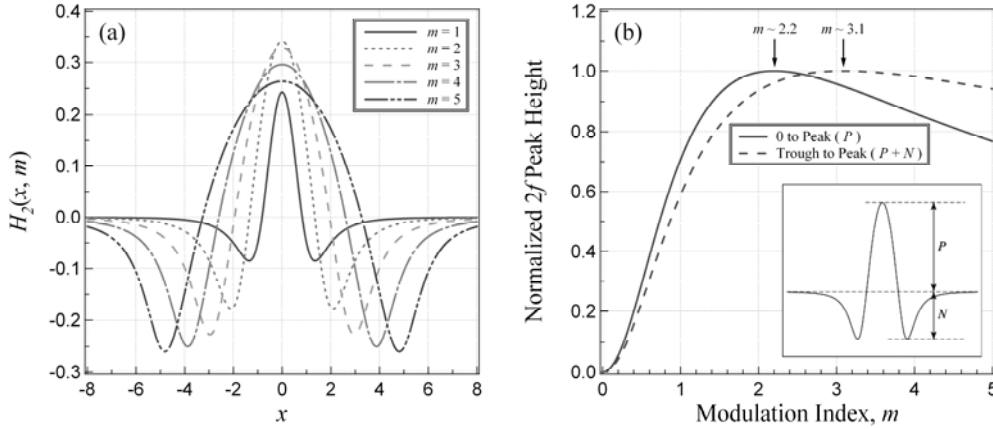


Figure 1 (a) Shape of $H_2(x, m)$ traces with different modulation indices m and (b) m -scale dependence of normalized $2f$ peak height and separation between peak and trough.

From Equations (13) and (14), the peak height P_{2f} at the center of the absorption spectrum ($\nu = \nu_0$, i.e. $x = 0$) can be written as

$$\frac{2(XL)PS}{\pi\Delta\nu_c} \frac{2}{m^2} \left(\frac{m^2+2}{\sqrt{m^2+1}} - 2 \right) \propto \frac{P_{2f}}{I_0} \quad (15)$$

Thus the concentration of the target gas XL is given as

$$XL \propto \frac{P_{2f}\Delta\nu}{I_0S} \left\{ \frac{2}{m^2} \left(\frac{m^2+2}{\sqrt{m^2+1}} - 2 \right) \right\}^{-1} \quad (16)$$

These treatments correspond to the strict solution by Cooper & Warren (1987).

For the measurement in an actual incinerator, there exist some adverse influences on the higher order harmonic signal of the absorption. The laser intensity could be unexpectedly fluctuated because the measuring circumstance is not ideal. Due to the nonuniform concentration, temperature and pressure distributions along the optical path, and also due to laser light attenuation by aerosol scattering and absorption other than the resonance absorption, the second harmonic signal is distorted. In the case of small background noise, the influence of the intensity fluctuation can be reduced using the DC component of the absorption signal.

3. COMBUSTION SYSTEM

FMS (WMS) is one of the promising candidates for measuring the gas component of exhaust flue in a waste incinerator. In a schematic drawing of a typical waste incinerator (Figure 2), the arrows indicate the gas flow through the whole incineration system, and the solid circles represent the recommended measuring points for FMS (WMS). Wastes gathered from households and industries are thrown from the left-hand side of the figure and burned at a temperature ranging from 800-1000 °C, and the ashes are collected at the bottom. The burned gas is cleaned and then the temperature is lowered to ~ 200 °C in order not to generate dioxin. After the injection of the chemical reagent such as calcium hydroxide to reduce the caustic component such as HCl, the dust is removed by the bag filters, and then the flue gas is released to the atmosphere through the chimney at the right-hand side.

Before releasing, or during the process of cleaning, the harmful components in the exhaust gas are monitored and controlled to observe the allowance limit of the emission. For the monitoring purposes, FMS (WMS) can be applied, especially for HCl, CO (carbon monoxide) and O₂ (oxygen) observations. The measurements of CO and O₂ are also useful for controlling the combustion efficiency.

4. OPTICAL PROPERTIES OF EXHAUST GAS

For the molecular spectroscopic database, HITRAN 2008 edited by Rothman et al., (2009) has been generally used. Figure 3 shows the distribution of the absorption bands of ¹⁶O₂, ¹²C¹⁶O and ¹H³⁵Cl as the function of wavelength in the NIR (near infrared) and the MIR (mid infrared) region. The ordinate shows the absorption strength at the reference temperature of $T_{\text{ref}} = 296$ K.

Though O₂ is a symmetric molecule, it has an absorption band near 760 nm (A-Band) due to the magnetic dipole interaction of its nuclear spin (Brown & Plymate, 2000). The rotational quantum number of the lower level N'' , and the upper level N' , are odd and even, respectively, so the spin quantum numbers are $S'' = 1$ for the lower state and $S' = 0$ for the upper state. Therefore, the total angular momentum, $J = N + S$ (N : rotational angular momentum, S : spin angular momentum), has three distinct energy levels for the lower state ($J'' = N'' - 1, N'', N'' + 1$) and only one level for the upper state ($J' = N'$). The notation of a rotational transition is expressed by the combination of $\Delta N N'' \Delta J J''$.

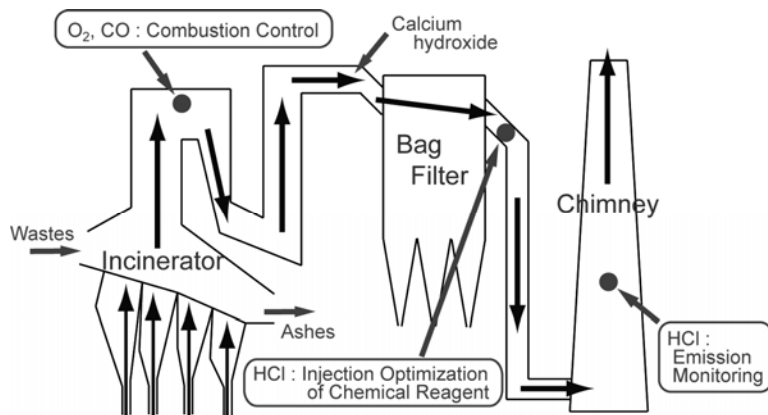


Figure 2 A schematic drawing of a typical waste incinerator

In Figure 3, for the vibrotational transitions of $^{12}\text{C}^{16}\text{O}$ and $^1\text{H}^{35}\text{Cl}$, $\Delta v (= v' - v'') = 1$ and $v'' = 0$ is the fundamental transition, where v' and v'' are respectively the upper state and the lower state vibrational quantum numbers. The transitions for $\Delta v \geq 2$ are the overtones. It is obvious that the absorption strength at the room temperature of the first overtone ($\Delta v = 2, v'' = 0$) and the second overtone ($\Delta v = 3, v'' = 0$) are one over several tens, and one over several thousands of that for the fundamental transition, respectively. So the observation of a fundamental transition is preferable. However, due to the commercial availability of LD light source, the absorption lines below the $2 \mu\text{m}$ wavelength region are commonly selected. According to this restriction, the first overtone band for HCl ($1.7\text{-}1.8 \mu\text{m}$), and the second overtone band for CO ($1.6 \mu\text{m}$) are generally used for monitoring by FMS (WMS).

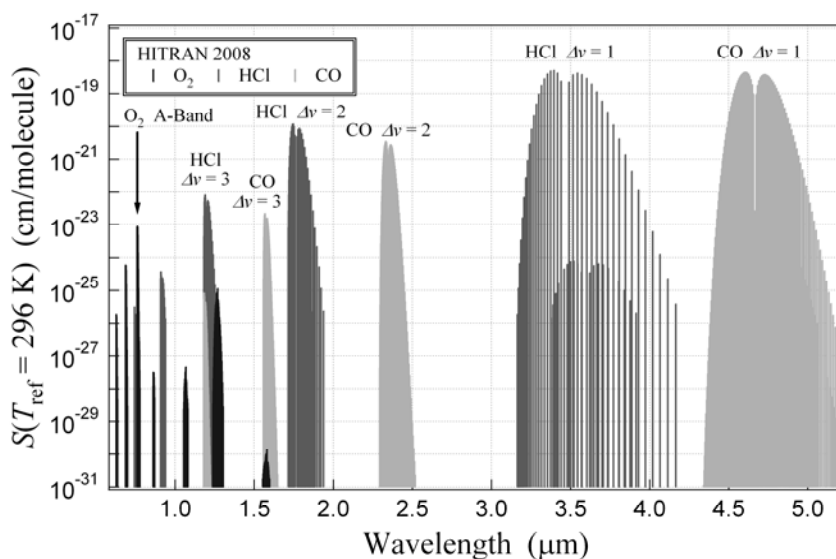


Figure 3 Distribution of absorption bands in NIR and MIR wavelength region for $^{16}\text{O}_2$, $^{12}\text{C}^{16}\text{O}$ and $^1\text{H}^{35}\text{Cl}$

Figure 4 shows the relationship between the rotational quantum number and the absorption strength $S(T_{\text{ref}})$ for the fundamental, first overtone and second overtone bands for HCl. The transitions for $\Delta J = -1$ correspond to the P-branch and are shown in the left-hand side of the figure, and $\Delta J = 1$ correspond to the R-branch on the right-hand side. In the first overtone band ($v' = 2 \leftarrow v'' = 0$), R2 transition ($\Delta J = 1, J'' = 2$) shows the strongest absorption strength, and the strength of R10 transition ($\Delta J = 1, J'' = 10$) is about 1/50 of that of R2. The observation of the R2 absorption line seems to be suitable for the monitoring of HCl concentration, but in an actual incinerator, a significant amount of water vapor exists and the H_2O absorption near the R2 absorption line of HCl could interfere with the HCl measurement. R3 transition ($\Delta J = 1, J'' = 3$) at $1.74238 \mu\text{m}$ is usually used instead of R2 transition because R3 transition shows the favorable absorption strength and is expected to be less affected by water vapor absorption than R2 transition.

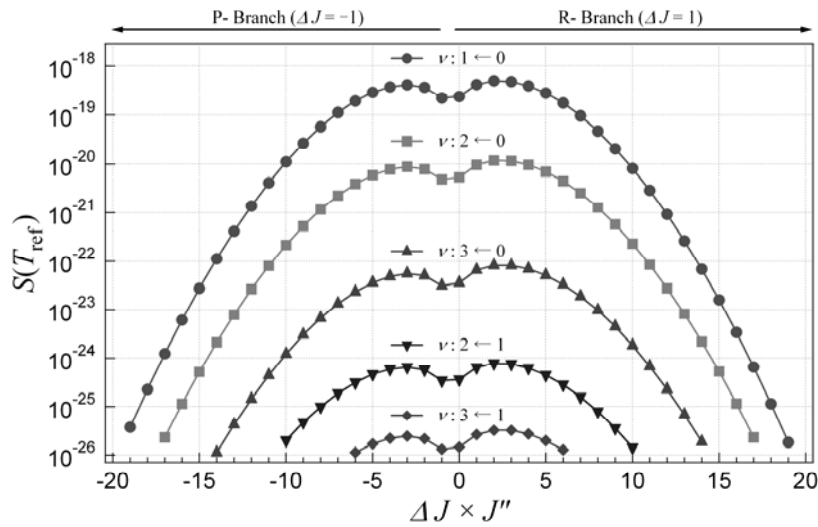


Figure 4 Rotational quantum number dependences of $S(T_{\text{ref}})$ for HCl. Horizontal axis shows rotational quantum number. $\Delta J = -1$ corresponds to P-branch, and $\Delta J = 1$ R-branch.

5. LABORATORY EXPERIMENT

The WMS measurement of the first overtone HCl absorption transition ($v' = 2 \leftarrow v'' = 0$, R3) at $1.74238 \mu\text{m}$ was performed in the laboratory of Kyoto Electronics Manufacturing Co., Ltd. To observe the intended absorption line, a temperature-stabilized DFB (distributed feedback) laser diode was used. The emission wavelength of the laser was scanned and modulated by controlling the injection current. HCl standard gas of a certain concentration was introduced to a test quartz cell with wedged windows. The optical path length of the test cell was designed to be 50 cm. The gas temperature inside the test cell was maintained from room temperature to 250°C (similar to the gas temperature at the chimney in a waste incinerator) by a controlled heating apparatus, and the gas temperature inside the test cell was measured by thermocouples. The absorption signal was detected by an InGaAs photodiode detector, and the second harmonic frequency signal was obtained by a lock-in amplifier.

An example of the experimental results is provided (Figure 5). The gas temperature variations of the second harmonic frequency signal are also illustrated (Figure 5(a)). The ordinate is the amplitude of the second harmonic frequency signal in the arbitrary scale, and the abscissa

corresponds to the wavelength. The full scale of the abscissa shown here approximately corresponds to the wavelength span of 0.15 nm. As the temperature of the flue gas increases, the peak height and the trough depth of the spectrum gradually decrease. The wavelength gap between two troughs represents the full-width of the absorption spectrum. A subtle narrowing effect was observed with the rise of the gas temperature. Figure 5(b) shows the temperature dependences of the observed peak height of the second harmonic frequency spectra (Figure 5(a)) and the simulated theoretical absorption strength based on the HITRAN 2008 database (Rothman et al., 2009). Both data sets are normalized by the value corresponding to the gas temperature of 23°C. As can be seen in the figure, a good agreement between the experimental data and simulation has been obtained. These results encourage the possibility of temperature compensation of the peak height of the second harmonic frequency signal, i.e., the concentration of the gas component of interest, when the gas temperature is simultaneously measured.

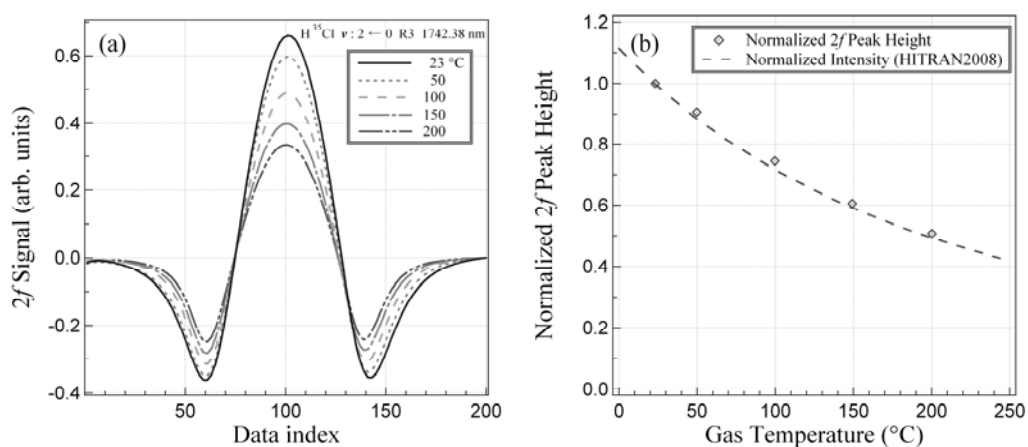


Figure 5 (a) Experimentally obtained temperature variations of second harmonic frequency signal of HCl R3 $v' = 2 \leftarrow v'' = 0$ transition at 1.74238 μm and (b) Comparison between experimental peak height of second harmonic spectrum and theoretical absorption strength simulated with HITRAN 2008 database (Rothman et al., 2009)

6. SUMMARY

In a waste incinerator, the concentration measurement of the combustion and the exhaust gas component under harsh environmental conditions such as high temperature, high pressure and high humidity has become increasingly important in order to monitor emission and control the combustion condition. The optical measurement methods are considered to be ideal for these purposes because these methods can intrinsically perform real-time, *in situ* and automated measurements. Among those optical methods, TDLAS based on FMS (WMS) is one of the most suitable methods.

In this paper, we described the approximated theory of FMS (WMS) on the assumption of the weak absorption. As an example of the experimental result to discuss the practical applicability of FMS (WMS), we demonstrated the temperature dependence of the second harmonic frequency signal of HCl absorption in the first overtone band. The experimental data show good agreement with the theoretical prediction based on the molecular spectroscopic database. This result encourages the possibility of the compensation method for the variation of the FMS

(WMS) signal due to the fluctuation of gas temperature. As described above, the FMS (WMS) signal could be affected by the measurement circumstance, such as temperature, pressure and humidity. To derive the absolute concentration of the gas component in the actual combustion field correctly, it is desirable to clarify and consider how the circumstance affects the FMS (WMS) signal.

The emission wavelength region of the cost-effective and practical laser light source to date is less than 3 μm . The quantum cascade lasers (QCL) or the interband cascade lasers (ICL) can reach the wavelength region of the fundamental vibrotational transitions. With increased availability and use of such lasers, the environmental gas concentration measurement based on TDLAS technique with high sensitivities will extend its applicability to the wide fields of the environmental monitoring.

7. ACKNOWLEDGMENT

The authors gratefully acknowledge to Associate Professor Tatsuo Shiina at graduate school of Chiba university for his helpful support for our laboratory experiment. The authors also would like to thank all technical staffs in Kyoto Electronics Manufacturing Co., Ltd.

8. REFERENCES

- Arndt, R., 1965. Analytical Line Shapes for Lorentzian Signals Broadened by Modulation, *Journal of Applied Physics*, Volume 36, Number 8, pp. 2522-2524.
- Brown, L.R. & Plymate, C., 2000. Experimental Line Parameters of the Oxygen a Band at 760 nm, *Journal of Molecular Spectroscopy*, Volume 199, Number 2, pp. 166-179.
- Cooper, D.E. and Warren, R.E., 1987. Frequency Modulation Spectroscopy with Lead-salt Diode Lasers: A Comparison of Single-tone and Two-tone Techniques, *Applied Optics*, Volume 26, Number 17, pp. 3726-3732.
- Reid, J. & Labrie, D., 1983. Second-harmonic Detection with Tunable Diode Lasers - Comparison of Experiment and Theory, *Applied Physics B: Lasers and Optics*, Volume 26, Number 3, pp. 203-210.
- Rothman, L.S., Gordon, I.E., Barbe, A., Benner, D.C., Bernath, P.F., Birk, M., *et al.*, 2009. The HITRAN 2008 Molecular Spectroscopic Database, *Journal of Quantitative Spectroscopy and Radiation Transfer*, Volume 110, Numbers 9-10, pp. 533-572.
- Silver, J.A., 1992. Frequency-modulation Spectroscopy for Trace Species Detection: Theory and Comparison among Experimental Methods, *Applied Optics*, Volume 31, Number 6, pp. 707-717.
- Uehara, K., 1998. Dependence of Harmonic Signals on Sample-gas Parameters in Wavelength-modulation Spectroscopy for Precise Absorption Measurements, *Applied Physics B: Lasers and Optics*, Volume 67, Number 4, pp. 517-523.
- Wahlquist, H., 1961. Modulation Broadening of Unsaturated Lorentzian Lines, *Journal of Chemical Physics*, Volume 35, Number 5, pp. 1708-1710.
- Wilson, G.V.H., 1963. Modulation Broadening of NMR and ESR Line Shapes, *Journal of Applied Physics*, Volume 34, Number 11, pp. 3276-3285.